

Magnetorotational-type Instability in Couette–Taylor Flow of a Viscoelastic Polymer Liquid

Gordon I. Ogilvie* and Adrian T. Potter

*Department of Applied Mathematics and Theoretical Physics, University of Cambridge,
Centre for Mathematical Sciences, Wilberforce Road, Cambridge CB3 0WA, UK*

(Dated: April 25, 2022)

We describe an instability of viscoelastic Couette–Taylor flow that is directly analogous to the magnetorotational instability (MRI) in astrophysical magnetohydrodynamics, with polymer molecules playing the role of magnetic field lines. By determining the conditions required for the onset of instability and the properties of the preferred modes, we distinguish it from the centrifugal and elastic instabilities studied previously. Experimental demonstration and investigation should be much easier for the viscoelastic instability than for the MRI in a liquid metal. The analogy holds with the case of a predominantly toroidal magnetic field such as is expected in an accretion disk and it may be possible to access a turbulent regime in which many modes are unstable.

PACS numbers: 47.20.-k, 46.35.+z, 47.65.-d, 97.10.Gz

The magnetorotational instability (MRI) is widely regarded as one of the most important instabilities in astrophysics. It occurs in a differentially rotating fluid of sufficiently high electrical conductivity in the presence of a magnetic field, when the angular velocity decreases with distance from the axis of rotation. The MRI is especially relevant to astrophysical accretion disks, where it is believed to give rise to turbulence and angular momentum transport, but it can also occur in stellar interiors [1, 2, and references therein].

The mechanism of instability can be visualized by considering two fluid elements connected by magnetic field lines, which act as an elastic tether. The elements initially orbit at the same radius and one is displaced inward so that its angular velocity increases. Being retarded by the tether, it loses angular momentum and moves to a still smaller orbit so that the process runs away. Both inertial forces and high conductivity are important to the mechanism.

Experimental demonstration of the MRI is regarded as highly desirable but has proved difficult because of the need to achieve a sufficiently large magnetic Reynolds number ($Rm = LU\mu_0\sigma$, where L and U are characteristic length and velocity scales of the flow and σ is the electrical conductivity). Even for the most highly conducting liquid metals, the required Reynolds number ($Re = LU/\nu$, where ν is the kinematic viscosity) is extremely large, in excess of 10^6 .

A natural choice of experiment is the Couette–Taylor flow of a liquid metal between differentially rotating concentric cylinders. By setting the angular velocities of the cylinders in a “Keplerian” ratio, $\Omega \propto r^{-3/2}$, and introducing a uniform axial magnetic field, the MRI becomes possible while the centrifugal (inertial) instability is suppressed according to Rayleigh’s criterion [3]. The water prototype [4] of a planned experiment using liquid gallium [5] has attempted to deal with the strong end-effects that arise at large Re when the cylinders are not much

taller than the gap between them.

Behavior related to the MRI may have already been observed in a *spherical* Couette flow of liquid sodium [6]. The interpretation of this experiment is difficult because of the presence of hydrodynamic turbulence and a complicated pattern of differential rotation in the unmagnetized state. A different instability, which relies on the presence of a helical magnetic field, has also been reported in a cylindrical experiment [7, 8]. This result is controversial [9] and, since the instability occurs at $Rm \ll 1$, it does not resemble the MRI as conventionally understood.

In this Letter we describe an instability that is directly analogous to the MRI and occurs instead in a simple viscoelastic liquid, with polymer molecules playing the role of magnetic field lines. We suggest that an experiment to study this MRI analog would be much easier and may in some respects represent the astrophysical systems of interest more closely than liquid metal experiments.

The characteristic properties of magnetohydrodynamics (MHD) in the limit of large Rm are that the magnetic field lines are advected and distorted by the fluid flow and can be identified with material lines, and that the field exerts a tension through the Lorentz force. These two properties imply that the magnetic field imparts an elasticity to an electrically conducting fluid, which allows the propagation of Alfvén waves, for example.

Directly analogous behavior occurs in viscoelastic fluids such as dilute solutions of long-chain flexible polymer molecules in water or organic solvents. The polymer molecules also impart an elasticity to the fluid because they are advected and distorted by the flow and exert a tension. In earlier work [10] we drew attention to the physical and mathematical similarities between these situations. The mathematical viewpoint is that the force per unit volume is the divergence of a symmetric stress tensor which is Lie-transported by the fluid flow in the sense of a second-rank contravariant tensor field (its

upper-convected derivative is zero). This result applies asymptotically both to the (Maxwell) magnetic stress in MHD in the limit of large Rm and to the polymeric stress in the limit of large Deborah number ($De = S\tau$, where S is the shear rate and τ is the relaxation time of the fluid).

We also showed [10] that there is a direct analog of the MRI in rotating shear flows of a viscoelastic fluid, using a Cartesian model that can be considered as a local approximation of a Couette–Taylor flow when the rotation and shear rates are comparable. For $De \gg 1$ the polymeric tension is parallel to the flow and corresponds to an equivalent magnetic field also in that (azimuthal) direction. Growth rates and eigenfunctions of the viscoelastic and MHD problems were found to be very similar.

Here we present a new analysis of the linear stability of viscoelastic Couette–Taylor flow, applicable to an experiment with cylindrical geometry. By optimizing the growth rate over all wavenumbers, we determine the likely initial outcome of such an experiment. We also show how the MRI analog can be distinguished from other types of instability in the same system.

A viscoelastic fluid is governed by the equation of motion,

$$\rho \left(\frac{\partial \mathbf{u}}{\partial t} + \mathbf{u} \cdot \nabla \mathbf{u} \right) = -\nabla p + \nabla \cdot \mathbf{T} + \mu_s \nabla^2 \mathbf{u}, \quad (1)$$

the incompressibility condition, $\nabla \cdot \mathbf{u} = 0$, and, in the case of an Oldroyd-B fluid, the constitutive equation

$$\begin{aligned} \mathbf{T} + \tau \left[\frac{\partial \mathbf{T}}{\partial t} + \mathbf{u} \cdot \nabla \mathbf{T} - (\nabla \mathbf{u})^T \cdot \mathbf{T} - \mathbf{T} \cdot \nabla \mathbf{u} \right] \\ = \mu_p [\nabla \mathbf{u} + (\nabla \mathbf{u})^T]. \end{aligned} \quad (2)$$

Here ρ , p , and \mathbf{u} are the density, pressure, and velocity of the fluid, μ_s and μ_p are the solvent and polymer viscosities, and τ is the relaxation time of the polymeric stress \mathbf{T} . The widely adopted Oldroyd-B model is the simplest nonlinear description of a dilute polymer solution and can be derived directly from a kinetic model [11].

In the Couette–Taylor experiment the basic flow is $\mathbf{u} = r\Omega(r) \mathbf{e}_\phi$, where (r, ϕ, z) are cylindrical polar coordinates, $\Omega(r) = A + Br^{-2}$, and the constants A and B are such as to match the angular velocities $\Omega_{1,2}$ of the inner and outer cylinders of radii $r_{1,2}$. The polymeric stress components are $T_{r\phi} = -2\mu_p Br^{-2}$ and $T_{\phi\phi} = 8\mu_p \tau B^2 r^{-4}$, the latter being analogous to the “hoop stress” of a magnetic field $B_\phi = (\mu_0 T_{\phi\phi})^{1/2}$. End-effects should be unimportant provided that the height of the cylinders is much larger than the gap width $d = r_2 - r_1$.

Two dimensionless numbers associated with the experiment are the Reynolds number $Re = r_1 d |\Omega_2 - \Omega_1| / \nu$, which measures the relative importance of inertial and viscous effects (here $\nu = (\mu_s + \mu_p) / \rho$ is the total kinematic viscosity), and the Deborah number $De = r_1 |\Omega_2 - \Omega_1| \tau / d$, which quantifies the importance of elasticity.

We linearize equations (1) and (2) about the basic flow and seek solutions with the dependence $\exp(st + im\phi + ikz)$, obtaining a sixth-order system of ordinary differential equations for the radial structure of an eigenmode with complex growth rate s , integer azimuthal mode number m and real axial wavenumber k . No-slip boundary conditions apply at $r = r_{1,2}$.

We solve the problem by two independent methods. First, we apply Chebyshev collocation on a Gauss–Lobatto grid to convert the system into an algebraic generalized eigenvalue problem, which we solve directly using a LAPACK routine. Second, we use a shooting method based on a 4th/5th order Runge–Kutta integrator with adaptive stepsize. The two routines agree to very high precision. The Chebyshev method is useful for examining all the eigenmodes with a sufficiently simple radial structure to be adequately resolved (spurious modes are also generated which must be rejected). The shooting method is good for following a single mode as the parameters are varied.

At each point in the (De, Re) plane we seek to maximize the growth rate $Re(s)$ with respect to both m and k . Once the preferred wavenumbers are obtained at one point, the optimal solution is tracked through the plane, making the necessary adjustments to m and k .

Two different instabilities have previously been reported in viscoelastic Couette–Taylor flow [12]. One is the centrifugal (inertial) instability (CI) of Rayleigh and Taylor [3], which occurs at sufficiently large Re even in the Newtonian limit ($De = 0$). The other is the purely elastic instability (EI) of Muller et al. [13] and Larson et al. [14], which occurs at sufficiently large De even in the inertialess limit ($Re = 0$). The CI is driven by shear energy and requires the specific angular momentum $|r^2 \Omega|$ to decrease with r , while the EI is driven by elastic energy and simply requires shear and curved streamlines.

The MRI analog, however, depends on both elasticity and inertial forces, and therefore requires both Re and De to be sufficiently large. It is driven by shear energy and requires the angular velocity $|\Omega|$ to decrease with r [3].

We tested our methods by reproducing standard results on the CI of a Newtonian fluid and also the results of Ref. [10] in the limit of a narrow gap.

We made strenuous efforts to reproduce the results of Ref. [15], where a problem identical to ours was considered in a different parameter regime, but we obtained only qualitative agreement with many of their findings. To verify our own results we derived the linearized equations by two independent methods and also obtained matching numerical results with completely independent codes.

For the purposes of illustration we adopt the parameters $r_1/r_2 = 0.95$ and $\mu_s/\mu_p = 1$. The latter ratio could be either small or large in practice, depending on the choice of solvent. Boger fluids, which avoid shear

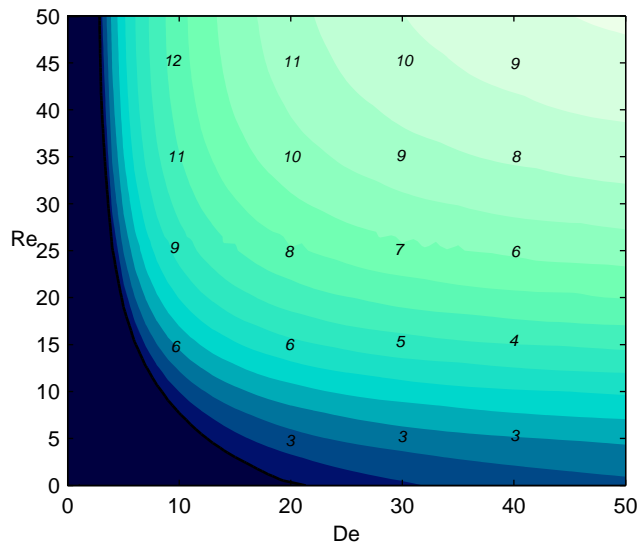


FIG. 1: Contours of the growth rate $\text{Re}(s)/\Omega_1$, optimized with respect to m and k , for case 1 ($p = -3/2$). Contour values increase from 0 to 0.35 in steps of 0.025 starting from the thick line (negative contours are not plotted). The preferred azimuthal mode number m is indicated by numerals.

thinning and conform more accurately to the Oldroyd-B model, have more viscous solvents.

We set the angular velocities of the cylinders in the ratio $\Omega_2/\Omega_1 = (r_2/r_1)^p$, with $p = -3/2$ (case 1), $p = +3/2$ (case 2) or $p = -3$ (case 3). Case 1 (a Keplerian ratio) should exhibit both EI and MRI, case 2 only EI, and case 3 all three instabilities.

In Fig. 1 we show the optimized growth rate in the (De, Re) plane for case 1. The EI is seen at $\text{Re} = 0$ for $\text{De} > 19$; it prefers a small value of m and its growth rate is limited here to $< 0.1 \Omega_1$. As Re is increased, instability occurs for a much wider range of De and with larger growth rates. This is the MRI analog. The preferred value of m increases with Re/De as the equivalent magnetic field becomes weaker [10]. The EI prefers a larger value of k . As expected, the CI is absent and there is no instability in the Newtonian limit $\text{De} = 0$.

A typical eigenfunction of the MRI analog at the onset of instability is shown in Fig. 2. This solution is qualitatively similar to Taylor vortices and has a vertical wavelength comparable to the gap width but is nonaxisymmetric and would appear as a rotating spiral pattern. However, nonlinear pattern selection may favor a linear combination of upward and downward spirals, resulting in a “ribbon” structure.

In case 2 (Fig. 3) the ratio of shear to rotation is similar to case 1 but of opposite sign, so that the MRI and CI are absent. We find that the EI operates in a very similar fashion at small Re but is suppressed by increasing Re at fixed De . A comparison of Figs 1 and 3 makes it clear that only the very low- Re behavior in Fig. 1 can be

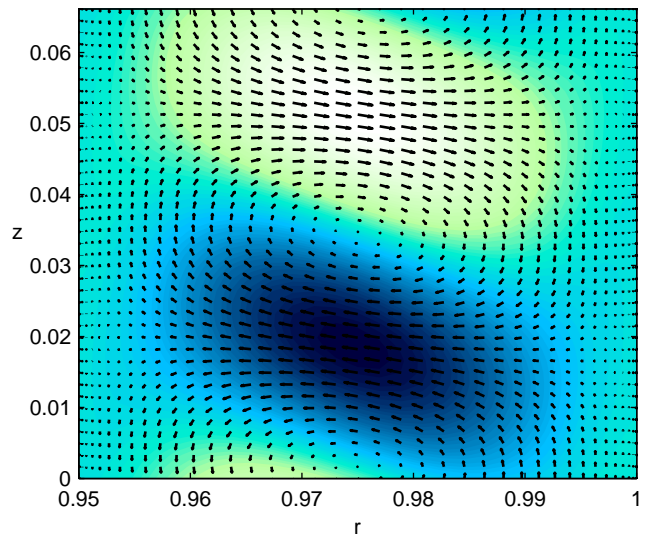


FIG. 2: Eigenfunction of the preferred mode in case 1 at the onset of instability for $(\text{De}, \text{Re}) = (3.3, 40)$, where $(m, k) = (11, 95)$. The azimuthal velocity perturbation is indicated by color/grayscale. One vertical wavelength is shown.

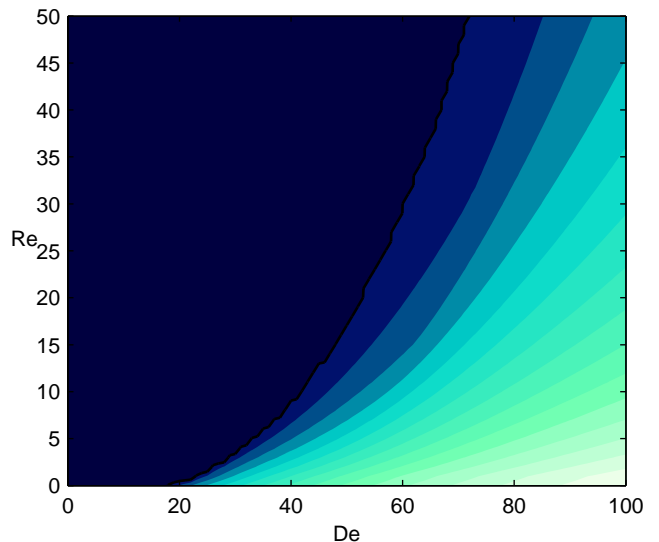


FIG. 3: Growth rate for case 2 ($p = +3/2$). Contour values increase from 0 to 0.07 in steps of 0.005. The preferred value of m is 2 throughout. Note the different horizontal scale.

attributed to the EI.

In case 3 (Fig. 4) we observe similar behavior to case 1 in much of the (De, Re) plane. However, the CI is seen operating at small De for $\text{Re} > 85$, where it prefers $m = 0$ (the classic axisymmetric Taylor vortices). Fig. 4 therefore illustrates EI, MRI, and CI, but most of the unstable region can be identified as MRI by comparison with Figs 1 and 3. The growth rates and preferred mode numbers of the MRI are somewhat different from case 1 because of the different ratio of shear to rotation. We

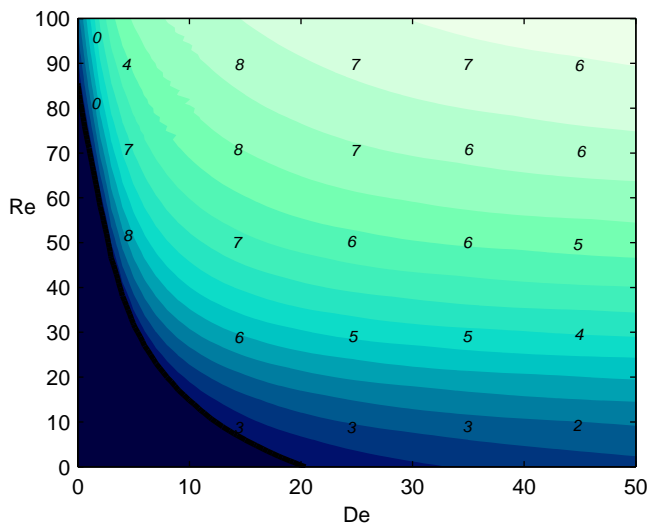


FIG. 4: Growth rate for case 3 ($p = -3$). Contour values increase from 0 to 0.7 in steps of 0.05. Note the different vertical scale.

find that the three instabilities are described by a mode that changes its character in a continuous way across the parameter space.

Experimental and theoretical studies of instabilities in viscoelastic Couette–Taylor flow have been carried out since the 1960s but have not revealed the three types of characteristic behavior seen here. The MRI analog is exhibited most clearly, as in our case 1, when the angular velocity decreases outward while the angular momentum increases. The few experiments in which the inner and outer cylinders can rotate independently (e.g., [16]) appear not to have examined this regime.

Previous studies have described either a reduction of the critical Re for the CI as De is increased [12, and references therein] or a reduction of the critical De for the EI as Re is increased [17]. The physical nature of this intermediate “inertioelastic mode” has not been discussed. A similar behavior can be seen in case 3 (Fig. 4) but we interpret it as the MRI analog. The MRI tends to dominate the CI when both the angular velocity and the angular momentum decrease outward, unless De is small. In case 2 (Fig. 3), where the MRI is absent, increasing Re tends instead to suppress the EI.

An experimental study of the MRI analog would require a standard Couette–Taylor apparatus and a suitable polymer solution. The polymer viscosity and relaxation time can be adjusted by varying the concentration of the solution. Care must be taken to maintain the temperature of the fluid in the presence of viscous dissipation. Some effects such as shear-thinning in lower-viscosity solvents may require the use of a more sophisticated constitutive model than Oldroyd-B. Subcritical, hysteretic behavior has been reported in viscoelastic Couette–Taylor flow [17, 18] and this may also affect the experimental

manifestation of the MRI analog.

The asymptotic nature of the analogy between viscoelastic and MHD flows [10] means that it is more accurate for larger values of Re and De . At the onset of instability, as in Fig. 2, the analogy is good but not perfect. It is better in the upper right part of Fig. 1, where many modes are unstable and the flow may become turbulent. This situation would be analogous to a turbulent accretion disk containing a predominantly toroidal magnetic field. In contrast, liquid metal MRI experiments employ an axial magnetic field and are not expected to be able to access a regime of MHD turbulence. In these respects the polymer experiment may offer a more faithful representation of the astrophysical systems of interest. Other major advantages are that the materials are cheap and safe, and that optical visualization or velocimetry can be carried out.

This work was supported in part by STFC.

* Electronic address: gio10@cam.ac.uk

- [1] S. A. Balbus and J. F. Hawley, *Rev. Mod. Phys.* **70**, 1 (1998).
- [2] S. A. Balbus, *Annu. Rev. Astron. Astrophys.* **41**, 555–(2003).
- [3] S. Chandrasekhar, *Hydrodynamic and Hydromagnetic Stability* (Clarendon Press, Oxford, 1961).
- [4] H. Ji, M. Burin, E. Schartman and J. Goodman, *Nature* **444**, 343 (2006).
- [5] W. Liu, J. Goodman and H. Ji, *Astrophys. J.* **643**, 306 (2006).
- [6] D. R. Sisan, N. Mujica, W. A. Tillotson, Y.-M. Huang, W. Dorland, A. B. Hassam, T. M. Antonsen, and D. P. Lathrop, *Phys. Rev. Lett.* **93**, 114502 (2004).
- [7] R. Hollerbach and G. Rüdiger, *Phys. Rev. Lett.* **95**, 124501 (2005).
- [8] F. Stefani, T. Gundrum, G. Gerbeth, G. Rüdiger, M. Schultz, J. Szklarski and R. Hollerbach, *Phys. Rev. Lett.* **97**, 184502 (2006).
- [9] W. Liu, J. Goodman, I. Herron and H. Ji, *Phys. Rev. E* **74**, 056302 (2006).
- [10] G. I. Ogilvie and M. R. E. Proctor, *J. Fluid Mech.* **476**, 389 (2003).
- [11] R. B. Bird, C. F. Curtiss, R. C. Armstrong and O. Hassager, *Dynamics of Polymeric Liquids*, 2nd Edn, vol. 2 (Wiley, New York, 1987).
- [12] R. G. Larson, *Rheologica Acta* **31**, 213 (1992).
- [13] S. J. Muller, R. G. Larson and E. S. G. Shaqfeh, *Rheologica Acta* **28**, 499 (1989).
- [14] R. G. Larson, E. S. G. Shaqfeh and S. J. Muller, *J. Fluid Mech.* **218**, 573 (1990).
- [15] M. Avgousti and A. N. Beris, *J. Non-Newtonian Fluid Mech.* **50**, 225 (1993).
- [16] B. M. Baumert and S. J. Muller, *Phys. Fluids* **9**, 566 (1997).
- [17] A. Groisman and V. Steinberg, *Europhys. Lett.* **43**, 165 (1998).
- [18] D. G. Thomas et al., *J. Non-Newtonian Fluid Mech.* **138**, 111 (2006).